SUBMITTED TO *the Astrophysical Journal*
Preprint typeset using LaTeX style emulateapj v. 10/09/06



# AN ORPHAN IN THE "FIELD OF STREAMS"

V. Belokurov[1], N. W. Evans[1], M. J. Irwin[1], D. Lynden-Bell[1], B. Yanny[2], S. Vidrih[1], G. Gilmore[1], G. Seabroke[1], D. B. Zucker[1], M. I. Wilkinson[1], P. C. Hewett[1], D. M. Bramich[1], M. Fellhauer[1], H. J. Newberg[3], R. F. G. Wyse[4], T. C. Beers[5], E. F. Bell[6], J. C. Barentine[7], J. Brinkmann[7], N. Cole[3], K. Pan[7], D. G. York[8]

SUBMITTED TO *the Astrophysical Journal*

## ABSTRACT

We use Sloan Digital Sky Survey Data Release 5 photometry and spectroscopy to study a tidal stream that extends over $\sim 50^\circ$ in the North Galactic Cap. From the analysis of the path of the stream and the colors and magnitudes of its stars, the stream is $\sim 20^{+7}_{-5}$ kpc away at its nearest detection (the celestial equator). We detect a distance gradient – the stream is farther away from us at higher declination. The contents of the stream are made up from a predominantly old and metal-poor population that is similar to the globular clusters M13 and M92. The integrated absolute magnitude of the stream stars is estimated to be $M_r \sim -7.5$. There is tentative evidence for a velocity signature, with the stream moving at $\sim -40$ kms$^{-1}$ at low declinations and $\sim +100$ kms$^{-1}$ at high declinations. The stream lies on the same great circle as Complex A, a roughly linear association of HI high velocity clouds stretching over $\sim 30^\circ$ on the sky, and as Ursa Major II, a recently discovered dwarf spheroidal galaxy. Lying close to the same great circle are a number of anomalous, young and metal-poor globular clusters, including Palomar 1 and Ruprecht 106.

*Subject headings:* galaxies: kinematics and dynamics — galaxies: structure — Local Group — Sagittarius dSph – Milky Way:halo

## 1. INTRODUCTION

The Sloan Digital Sky Survey (SDSS) (York et al. 2000) is an imaging and spectroscopic survey that has now mapped over 1/4 of the sky. It has already proven to be a powerful tool for the identification of Galactic substructure. For example, Newberg et al. (2002) and Yanny et al. (2003) identified a ring at low Galactic latitude, often called "the Monoceros Ring". It spans over $100^\circ$ in the sky (see also Ibata et al. 2003; Rocha-Pinto et al. 2003), but its progenitor remains unclear (Penarrubia et al. 2005). Odenkirchen et al. (2001) used SDSS data to find the spectacular $10^\circ$ tidal tails around the sparse and disrupting Galactic globular cluster Pal 5. More recently still, Belokurov et al. (2006a) found $4.5^\circ$ tails around the high-latitude globular cluster NGC 5466, while Grillmair & Dionatos (2006) discovered a $63^\circ$ tail that presumably arises from a so far unidentified globular cluster.

The best known example of a stream is the tidally stripped stars and globular clusters associated with the Sagittarius dwarf spheroidal. A panorama of the the Sagittarius stream in the Northern hemisphere was recently obtained by Belokurov et al. (2006b), who mapped out the stars satisfying $g - r < 0.4$ in almost all of SDSS Data Release 5 (DR5). This color plot of the high-latitude Galactic northern hemisphere has been dubbed the "Field of Streams". In addition to the features associated with the Sagittarius dSph, the plot exhibits extensive substructure. The purpose of this paper is to analyze the "Orphan Stream" – so named for its lack of obvious progenitor. This is a striking feature discovered by Belokurov et al. (2006b) in the Field of Streams, and independently detected in public SDSS data by Grillmair (2006).

## 2. MORPHOLOGY OF THE ORPHAN STREAM

SDSS imaging data are produced in five photometric bands, namely $u$, $g$, $r$, $i$, and $z$ (see e.g., Fukugita et al. 1996; Hogg et al. 2001; Smith et al. 2002; Gunn et al. 2006). The data are automatically processed through pipelines to measure photometric and astrometric properties and to select targets for spectroscopic follow-up (Lupton, Gunn, & Szalay 1999; Stoughton et al. 2002; Pier et al. 2003; Ivezić et al. 2004; Adelman-McCarthy et al. 2006). To correct for Galactic reddenning, we use the maps of Schlegel, Finkbeiner, & Davis (1998). All the magnitudes in the paper are reddenning corrected. Data Release 5 covers $\sim 8000$ square degrees around the Galactic North Pole, and 3 strips in the Galactic southern hemisphere.

The left panel of Figure 1 shows the Orphan Stream in an RGB composite image. It has been constructed using all SDSS DR5 stars [9] with $20.0 < r < 22.0$, with blue for stars with $0.0 < g-r \leq 0.2$, green for stars with $0.2 < g-r \leq 0.4$

[1] Institute of Astronomy, University of Cambridge, Madingley Road, Cambridge CB3 0HA, UK;vasily,nwe,mike@ast.cam.ac.uk
[2] Fermi National Accelerator Laboratory, P.O. Box 500, Batavia, IL 60510
[3] Rensselaer Polytechnic Institute, Troy, NY 12180
[4] The Johns Hopkins University, 3701 San Martin Drive, Baltimore, MD 21218
[5] Department of Physics and Astronomy and Joint Institute for Nuclear Astrophysics, Michigan State University, East Lansing, MI 48824
[6] Max Planck Institute for Astronomy, Königstuhl 17, 69117 Heidelberg, Germany
[7] Apache Point Observatory, P.O. Box 59, Sunspot, NM 88349
[8] Department of Astronomy and Astrophysics, University of Chicago, Chicago, IL 60637
[9] A small number of Data Release 6 stars are used to ensure continuous photometric coverage of the Orphan Stream (c.f. Grillmair

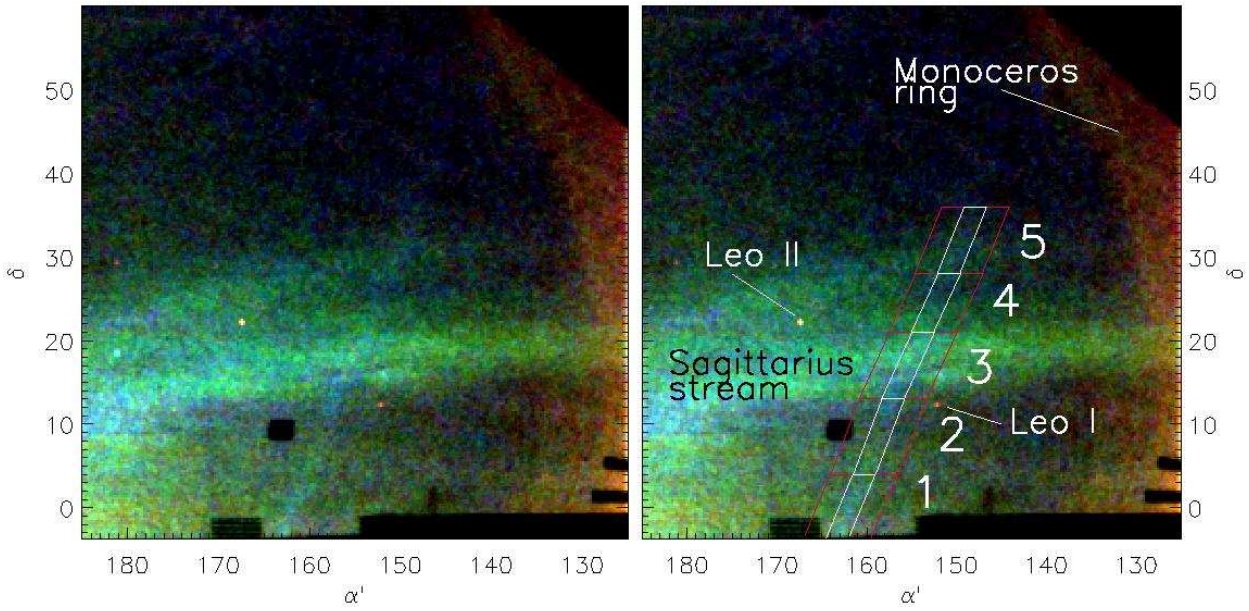


FIG. 1.— Left: A false color RGB composite of density of stars with $20.0 < r < 22.0$. Blue corresponds to $0.0 < g - r \leq 0.2$, green $0.2 < g - r \leq 0.4$ and red $0.4 < g - r \leq 0.6$. Right: The Sagittarius and Monoceros structures are marked, together with the on-stream and off-stream fields along the Orphan Stream. Also shown is the location of the recently-discovered probable globular cluster Segue 1 (Belokurov et al. 2006c). The black curves mark the limits of the DR5 spectroscopic footprint.

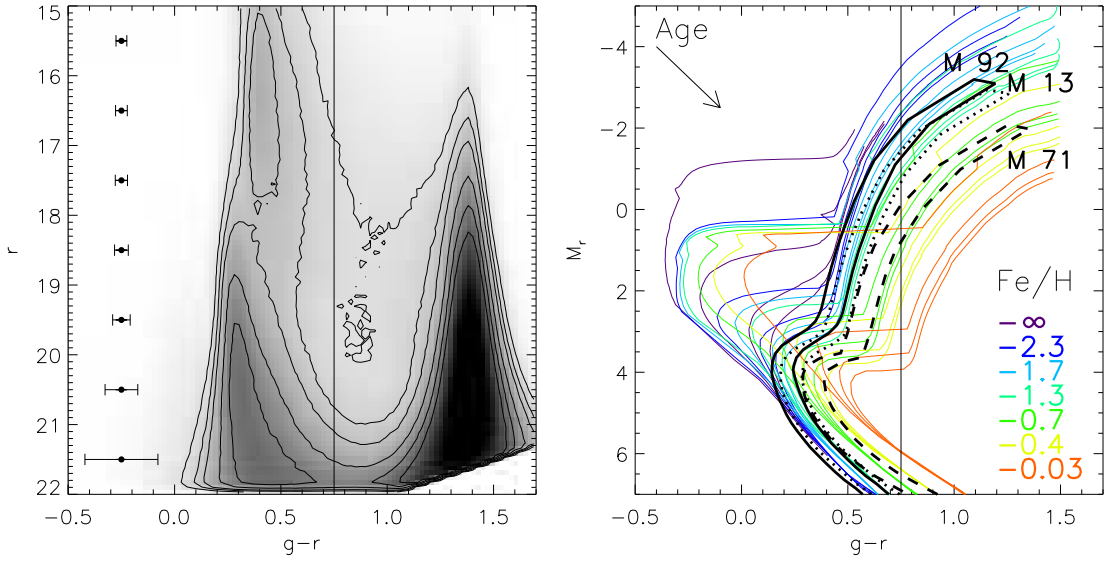


FIG. 2.— Left: Hess diagram for all stars in DR5. The typical errors in color are shown as a column of error bars on the left of the plot. The vertical line shows the color cut to constrain the population to blue stars. Right: Isochrones from Girardi et al. (2004), with different colors corresponding to different metallicities. Four representative ages are shown for each metallicity (1, 5, 10 and 14 Gyrs, left to right). Masks based on the ridgelines of M92 (solid), M13 (dotted) and M71 (dashed) from Clem (2005) are also shown.

and red for stars with $0.4 < g - r \leq 0.6$. The Orphan Stream is clearly visible running roughly from top to bottom at right ascensions $\alpha \approx 150° - 165°$. It may be traced over nearly 50° of arc in DR5. Some familiar objects are marked in the right panel of Figure 1, including the bifurcated Sagittarius stream, the Monoceros Ring, the newly discovered globular cluster Segue 1 (Belokurov et al. 2006c) and the two distant dwarf spheroidal galaxies Leo I and Leo II. On moving from lower to higher declinations, the stream becomes less detectable.

## 3. DISTANCES AND STELLAR POPULATIONS OF THE ORPHAN STREAM

Our aim is to constrain the distance and the stellar content of the Orphan Stream by comparison with CMDs of populations of known age and metallicity. For this purpose, we create masks (or color-magnitude boxes) based on the $r$ versus $g-r$ ridgeline of globular clusters and theoretical isochrones by shifting them both horizontally and vertically.

2006b, who used Data Release 4 only).

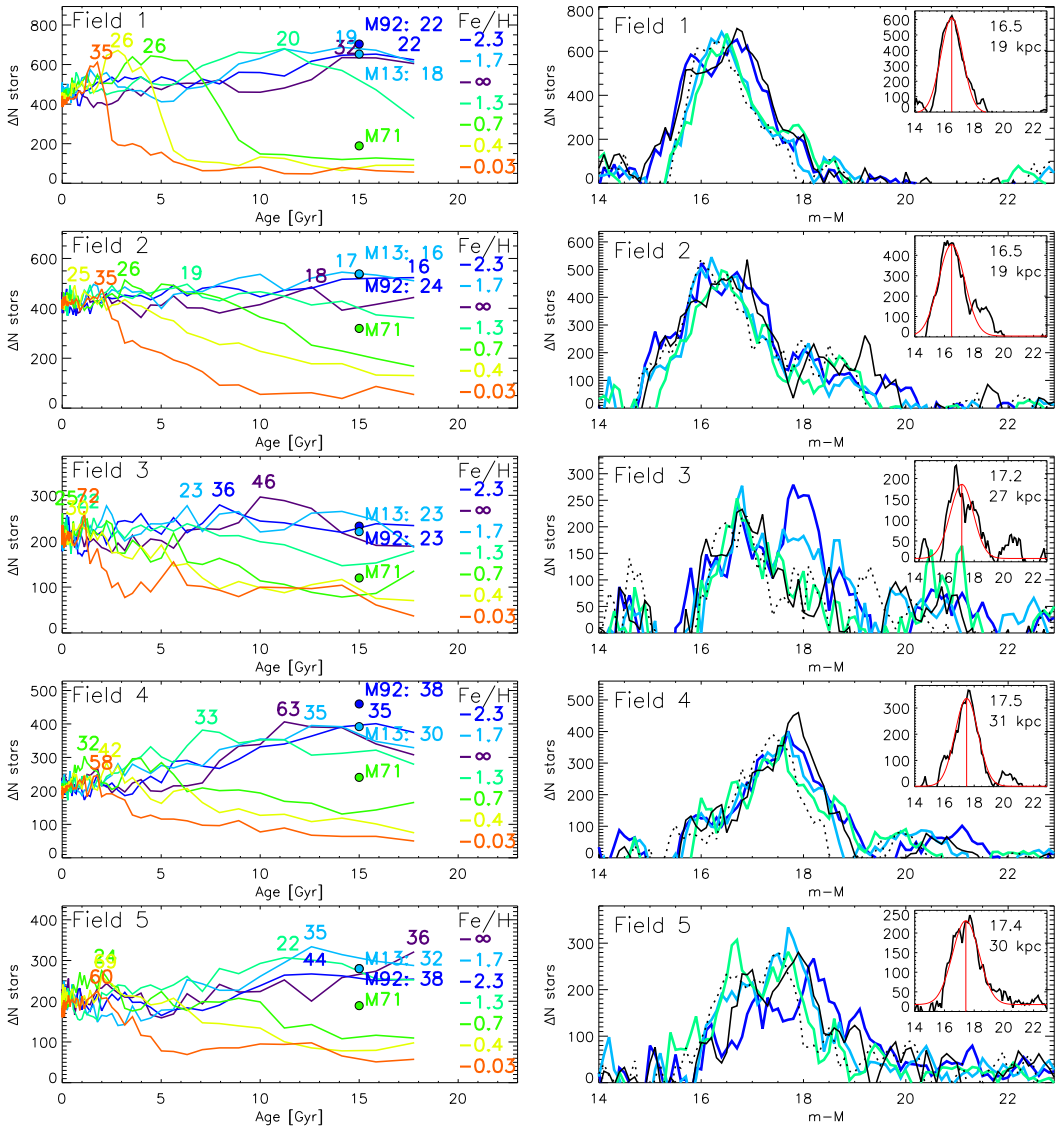


FIG. 3.— Left: For each field, the excess of stars in the Orphan Stream is shown as a function of age for different metallicities. Each point on the curve gives the maximum number of excess stars over all distance moduli. The peak of each curve gives the maximal signal for a given metallicity and is marked with its corresponding distance. It is apparent that there is a trade-off between age, metallicity and distance. Although there is a degeneracy, old metal-poor populations perform slightly better than young metal-rich ones. The filled circles show the signal picked up by the ridgeline masks for the three clusters M92, M13 and M71. Right: For three metal-poor populations ([Fe/H] $= -2.3, -1.7, -1.3$), we show the excess stars as a function of distance modulus for the age at the peak of the curve in the left panel. Also shown as solid and dotted lines are the curves using the ridgelines for M92 and M13. The inset shows the average of the five curves, together with a Gaussian fit in red. The number gives the central value of the Gaussian, which is our best estimate for the distance modulus, and hence the distance in kpc.

The mask is applied to select stars from the fields on and off the stream shown in the right panel of Figure 1. The signal is assessed by measuring the difference in the number of stars between the on and off streams as a function of distance modulus.

The left panel of Figure 2 shows a Hess diagram using all the stars in DR5. From blue to red, the main components of this CMD are the halo, thick disk and thin disk of the Milky Way. The vertical line shows a color cut at $g-r = 0.75$ used to minimise contamination from the disc stars. The right panel shows a sequence of theoretical isochrones computed by Girardi et al. (2004) for the SDSS photometric system. Different metallicities are distinguished by different colors as shown in the key to the panel. Although we investigate a range of ages, only the isochrones corresponding to 1, 5, 10 and 14 Gyrs are displayed. To compare the model predictions with observations, we also use the illustrated masks based on the ridgelines of the old (14 Gyrs) clusters M92 ([Fe/H] $= -2.2$), M13 ([Fe/H] $= -1.6$) and M71 ([Fe/H] $= -0.7$). These are produced from the data of Clem (2005) and chosen to span a representative range of metallicities.

The Orphan Stream (and parts of the Sagittarius stream) shown in Figure 1 are blue-green in our RGB scheme. This corresponds to $g-r \sim 0.3$, which is typical for the old, metal-poor halo. Most of the stars are redwards of $g-r \sim 0.2$. The stars that are bluewards could be either blue stragglers/blue horizontal branch stars, or main sequence turn-off stars scattered by large photometric errors.

TABLE 1
POSITIONS, DISTANCE MODULI AND DISTANCES OF THE ORPHAN STREAM.

| Field | $\alpha$ | $\delta$ | $m-M$ | $D$ |
|---|---|---|---|---|
| 1 | $162.1^\circ$ | $-0.5^\circ$ | $(16.5 \pm 0.1) \pm 0.7$ | $(20 \pm 1)^{+7}_{-5}$ kpc |
| 2 | $158.9^\circ$ | $8.5^\circ$ | $(16.5 \pm 0.1) \pm 0.9$ | $(20 \pm 1)^{+10}_{-7}$ kpc |
| 3 | $155.4^\circ$ | $17.0^\circ$ | $(17.1 \pm 0.1) \pm 0.7$ | $(26 \pm 1)^{+10}_{-7}$ kpc |
| 4 | $152.3^\circ$ | $25.0^\circ$ | $(17.5 \pm 0.1) \pm 0.8$ | $(32 \pm 1)^{+13}_{-10}$ kpc |
| 5 | $149.4^\circ$ | $32.0^\circ$ | $(17.5 \pm 0.1) \pm 0.9$ | $(32 \pm 1)^{+15}_{-12}$ kpc |

It is well-known that, given a color-magnitude diagram, simultaneously fitting for age, metallicity and distance modulus is degenerate. However, we have some clues as to the likely nature of the solution. The length and the width of the Orphan Stream suggests that it is dynamically old. If star formation ceased after the interaction that produced the tails, then the stars in the Stream are expected to be old. Also, when viewed from the Sun, tidal streams deviate from a great circle. The deviation is controlled by $\langle D \rangle / R_{\rm GC}$, where $\langle D \rangle$ is the stream's average heliocentric distance and $R_{\rm GC}$ is the offset of the Sun from the Galactic Center (here taken as 8 kpc). This parallactic effect gives an average heliocentric distance to the Stream of $\sim 15 \pm 5$ kpc.

The results of applying the masks to the photometric data are shown in Figure 3. In the left column, each panel corresponds to a different field. For a given metallicity and age, the masks are applied at different distance modulus and the number of excess stars in the on-stream field is calculated. The maximum value fixes a distance modulus. The number of excess stars at this distance modulus is used to build up the curve. The different colored lines correspond to different metallicities. Even though there is a degeneracy, the distances to which models of different metallicities converge are broadly consistent. For example, in Field 1, most of the distances are between 20 and 30 kpc, whereas in Field 5, they are mostly above 30 kpc. These values are somewhat higher than the $15 \pm 5$ kpc obtained from the parallactic effect, but consistent given the uncertainties and given the strong assumptions in the latter calculation. The M92 and M13 masks perform similarly to the corresponding isochrones, although there are some small discrepancies. It is reassuring that the results based on theoretical models are supported by those based on data.

Even though young stellar population seemingly perform quite well in Figure 3, this is not really the case. From the turn-off color of the Orphan Stream (see e.g., Figure 1), we can exclude young populations with a turn-off bluer than $g-r \sim 0.2$. Young isochrones are so blue that even the metal-rich ones extend blue enough to overlap with the Orphan Stream CMD and hence give a signal in Figure 3.

The general conclusion is that the old, metal-poor masks perform better, and in some instances, significantly better than the metal-rich masks. Given this, we take the three metal-poor models, namely [Fe/H] $= -2.2, -1.7, -1.3$, and identify the age at which the signal is maximised. These masks are now used to investigate the behavior of the signal as a function of distance modulus, shown in the panels in the right column. Also shown are the curves based on the ridgelines of M92 (solid) and M13 (dotted). They all show a similar performance and so we average them as displayed in the inset (solid black curve). A Gaussian model is then fit to this curve to give a central value, its uncertainty and a dispersion. These numbers are recorded in Table 1. The uncertainty in the mean gives a lower bound to the true distance error, whilst the dispersion overestimates the error, as the curves in the insets are a convolution of the true error distribution with the mask.

Grillmair (2006) has also recently analyzed the stars of the Orphan Stream. Grillmair's detection method uses M13 as a template for the stellar population of the stream. His Figure 3 shows a clear upper main sequence and sub-giant branch – which appear to be located somewhat blueward of the M13 ridgeline. This is consistent with a stream composed of a somewhat younger and/or metal-poor stellar population than M13. In turn, this is in agreement with the blue color of the Orphan Stream in our Figure 1, suggesting that our detection method is picking up primarily turn-off and upper main sequence stars.

Figure 4 shows the results of a search for blue horizontal branch (BHB) stars in the Orphan Stream. These are identified with the cut $g-r < 0.1$, and as usual the difference between on-stream and off-stream fields is computed. BHB stars have an absolute magnitude of $M_r = 0.75$ (see the right panel of Figure 2). Such a BHB population would be detected by peaks in the differential number distribution in the apparent magnitude range $16 < r < 18$ for the five fields inspected. There is no evidence for such a signal. However, blue stragglers have an absolute magnitude $M_r$ of between 2 and 4 and there are hints of peaks in fields 1 and 5 for $r \approx 20$. This seems consistent, given the distance moduli in Table 1.

## 4. ABSOLUTE MAGNITUDE AND WIDTH OF THE ORPHAN STREAM

Figure 5 shows cross-sections across the stream in a coordinate system which has been rotated so the stream lies along the $y$-axis. The cross-section contains only those stars with $g-r < 0.4$ and $21.0 < r < 22.0$. We estimate that the thickness (FWHM) of the Orphan Stream is $\sim 2^\circ$ in projection (or $\gtrsim 650$ pc assuming a conservative distance of $\sim 20$ kpc), which would make it broader than all known globular cluster streams, but smaller than the branches of the Sagittarius stream and the Monoceros Ring. This suggests that the progenitor was a low luminosity dwarf satellite galaxy, rather than a globular cluster.

Taking the total profile (upper curve in Figure 5), we fit a polynomial to estimate the background and then compute the luminosity of the stream. The number of excess stars in the $45^\circ$ arc of the stream is $\sim 4110$ within $160^\circ < x < 164^\circ$. Hence, the total apparent magnitude of the stream in these stars is around $r \sim 12$ (assuming an average $r$ magnitude

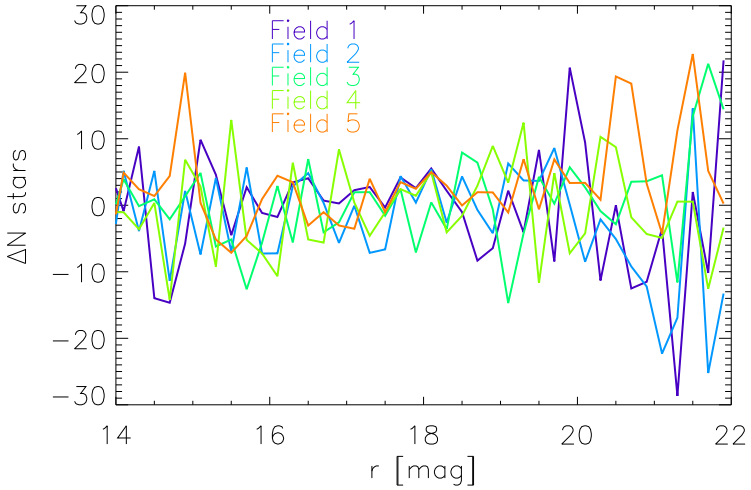


FIG. 4.— Differential histograms of number of stars with $g - r < 0.1$ as a function of apparent magnitude in different fields.

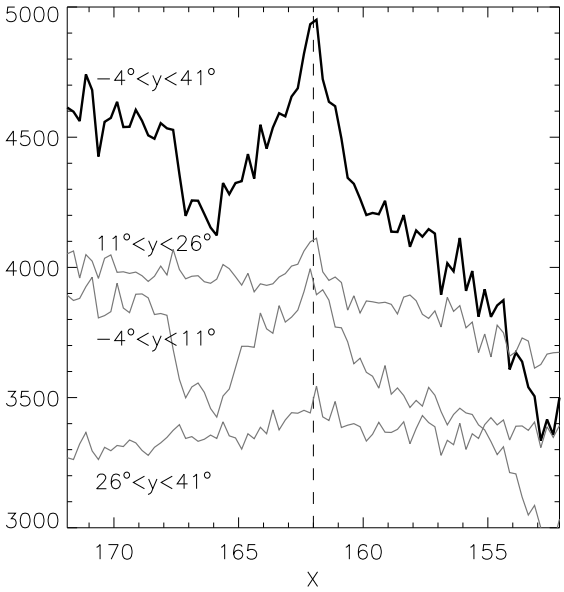


FIG. 5.— Profiles in stars with $g-r < 0.4$ and $21.0 < r < 22.0$ across the stream in a rotated coordinate system in which the stream lies along the $y$-axis. Notice that the peak of the profile barely shifts as we move along the stream.

of 21.0). Given the stream FWHM of $\sim 2°$, the average density of these stars is $\sim 45.6$ per square degree, which translates to an average surface brightness of the stream of $\sim 34\overset{m}{.}6$ per square arcsec. To correct for other stars, we use the data on the luminosity function of M92 derived from CFHT observations (Clem 2006, private communication). This gives the average surface brightness of the stream as $\sim 32\overset{m}{.}4$ per square arcsec and the total $r$ magnitude as $\sim 9.8$. Assuming the distance really is $\sim 20$ kpc gives an absolute magnitude of the 45° arc as $M_r \sim -6.7$ Assuming plausibly that there ought to be at least the same again on the other side of the progenitor, then we can boost the total to at least $M_r \sim -7.5$ for the stream stars alone. This number must be augmented by the (unknown) contribution from the progenitor nucleus, if it is still intact.

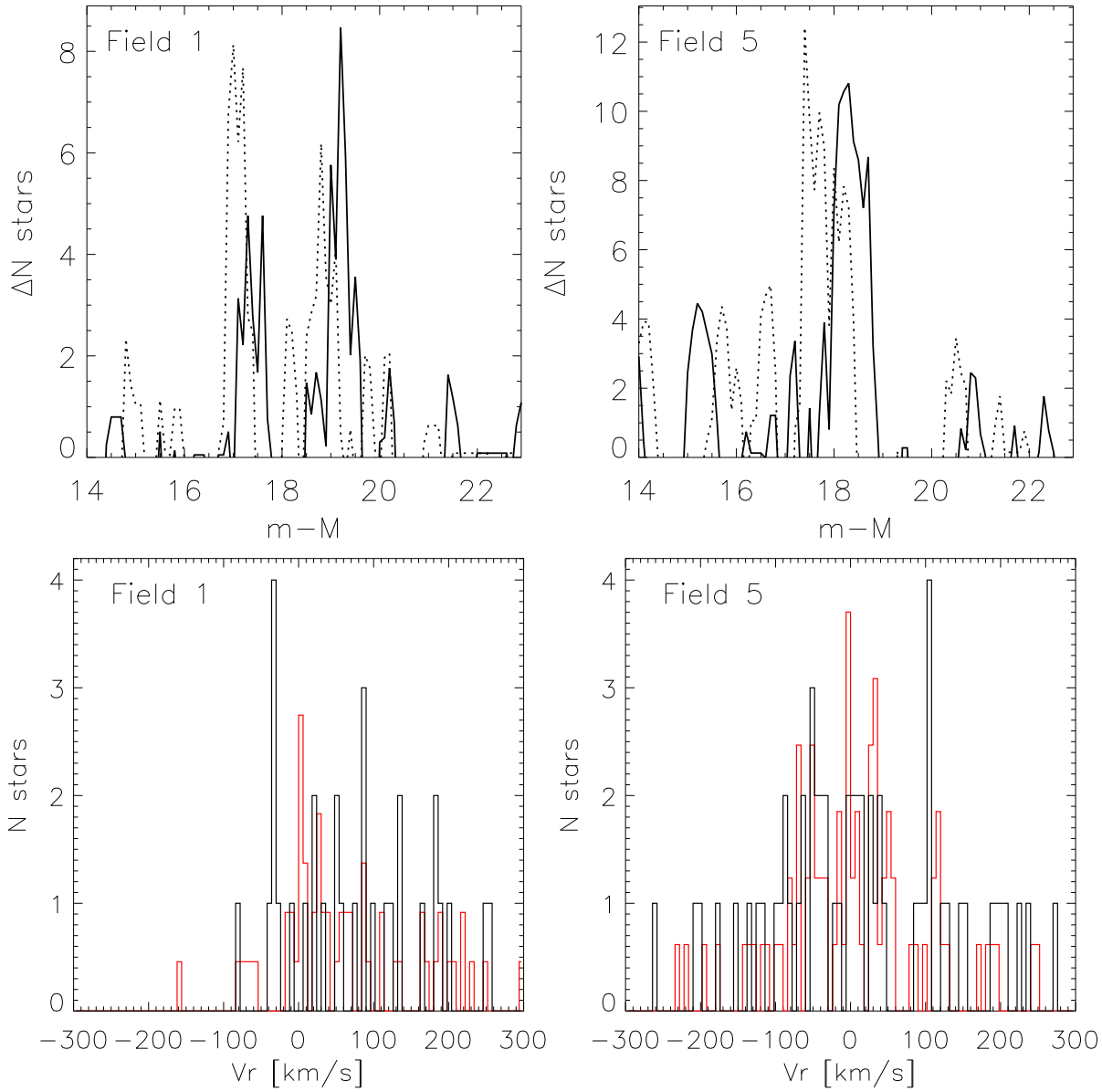


FIG. 6.— Upper: Excess number of stars in the on- and off-stream fields in the DR5 spectroscopic catalogue using the M92 (solid) and M13 (dotted) ridgeline masks. Even though the catalogue is much smaller, there is a reasonably clear detection of the Orphan Stream at a distance modulus of $\sim 17$. Lower: Velocity histograms of stars selected with the M92 and M13 ridgeline masks at the distance moduli satisfying $16.5 \leq m - M \leq 17.5$ in Field 1 and $17.5 \leq m - M \leq 18.5$ in Field 5. Black represents on-stream and red off-stream field stars.

## 5. VELOCITIES OF THE ORPHAN STREAM

The spectroscopic portion of SDSS DR5 covers 5713 deg$^2$ (Adelman-McCarthy et al. 2006). The outline of the spectroscopic footprint is shown as a black line in Figure 1. It does not cover Fields 3 and 4 of the Orphan Stream. The number of stars in the spectroscopic database is $\sim 215\,000$. Only stars brighter than $g \sim 20$ were targeted, and the selection algorithm is strongly non-uniform. A large number of spectra of standard stars were taken for calibration purposes. Other targets include K giants and dwarfs, F turn-off and subdwarf stars, as well as BHBs.

The accuracy of the radial velocities measured from the $R = 2000$ spectra obtained by the SDSS spectrographs vary from 7 km/s for the brighter stars ($r \sim 14$) to on the order of 20 km/s for the fainter stars ($r \sim 20$) (Allende Prieto et al. 2006), based on empirical tests. Information on the stellar atmospheric parameters ($T_{\rm eff}$, log g , [Fe/H]) for the DR5 stars with adequate spectra are presently being obtained by application of an automated spectroscopy analysis pipeline (Beers et al. 2006). This information will be utilized in future discussions of the Orphan Stream, once a comparison of the pipeline-derived atmospheric parameters with independently obtained high-resolution spectroscopy has been completed (Sivarani et al. 2005).

To test whether there is a signal of the Orphan Stream in the spectroscopic database, we apply the masks of M92 and M13 discussed earlier to the on- and off-stream fields. Given the faint magnitude cut-off, there are no turn-off

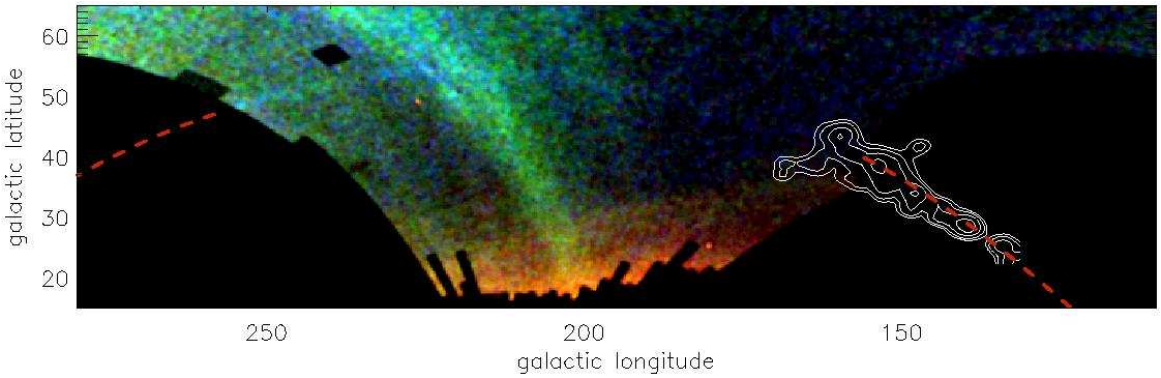


Fig. 7.— The Orphan Stream in Galactic coordinates $(\ell, b)$. Superposed on the map are the HI column densities of the Complex A association of High Velocity Clouds from Wakker (2001). Shown in red is a Galactocentric great circle fit assuming a orbit radius of $\sim 25$ kpc.

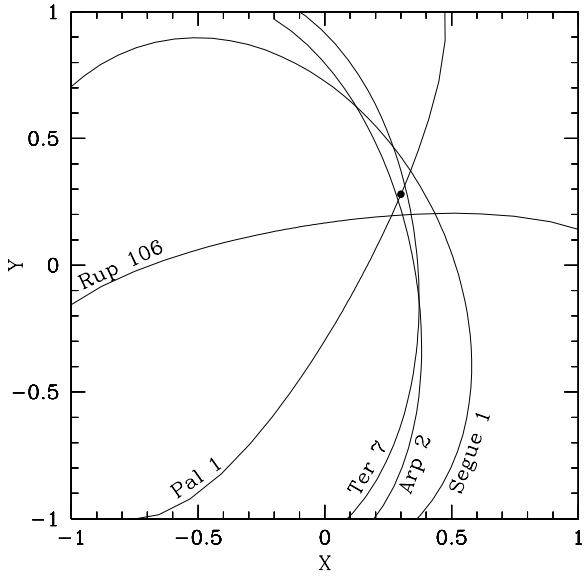


Fig. 8.— Polar paths of objects passing close to the pole of the Orphan Stream (marked by a filled circle).

stars belonging to the Stream in the database. So, our earlier algorithm is slightly changed to include a color cut designed to pick up giant branch stars. It is reassuring to see the peaks in the numbers of excess stars in the upper panel of Figure 6 at similar distance moduli to those reported in Table 1 for Fields 1 and 5 (no signal was detected in Field 2).

We now select stars using the masks of M92 and M13 placed at the distance moduli indicated by the peaks in the upper panels. Histograms of the velocities of these stars for the on and off stream fields are shown in black and red in the lower panels. A possible signature of the Orphan Stream is a peak in black without a corresponding peak in red. The largest peak in Field 1 is at $\sim -40$ kms$^{-1}$ and there is no signal in red. The largest peak in Field 5 is at $\sim 100$ kms$^{-1}$ and similarly there is a low signal in red. Bearing in mind the sparsity of the data, these detections are suggestive rather than conclusive.

## 6. THE GREAT CIRCLE OF THE ORPHAN STREAM

As pointed out by Lynden-Bell & Lynden-Bell (1995), tidal streams lie on great circles when viewed from the Galactic Center. The pole of the best fitting great circle is at $\ell_{\rm g} \approx 42°, b_{\rm g} \approx 55°$, where $(\ell_{\rm g}, b_{\rm g})$ are Galactic coordinates centered on the Galactic Center. Figure 7 shows the stream in Galactic coordinates $(\ell, b)$, together with the best fitting great circle. Superposed on the figures are the contours of HI column density of an association of High Velocity Clouds (HVCs) known as Complex A, taken from Wakker (2001). This is a stream of HI enshrouding seven clouds (A0 to AVI) and stretching $\sim 30°$ on the sky. The arc of neutral gas in Complex A runs along the same great circle as the optical stream. Complex A has a distance bracket 4.0 to 10.1 kpc, based on the presence or absence of absorption lines in the spectra of the stars AD UMa and PG 0859+593 (Wakker et al. 1996; van Woerden et al. 1999). Although Complex A is closer than the optical stream, it may still be associated and simply lie on a different wrap of the same

orbit. The velocities of the gas clouds in Complex A range from $-140$ to $-190$ kms$^{-1}$.

Very close to the great circle of the Orphan Stream and behind Complex A is the recently discovered, disrupting, dwarf spheroidal galaxy, Ursa Major II, or UMa II (Zucker et al. 2006, see also Grillmair (2006) who noted it as a stellar overdensity). This object lies at Galactic coordinates $\ell = 152.5°$, $b = 37.4°$. Its color-magnitude diagram exhibits a well-defined main sequence turn-off, from which its distance is estimated to be $\sim 30$ kpc, comparable to the distance of the Orphan Stream as it fades from view. Its radial velocity has not yet been measured.

Lynden-Bell & Lynden-Bell (1995) developed a method to identify possible globular clusters associated with a stream. Every possible pole of an object lies at right angles to its position vector (reckoned from the Galactic Center). The possible poles sweep out a great circle. Objects that can lie on the same orbit are identified as intersections in the paths of the poles of great circles. In practice, it is useful to plot the polar paths in the coordinates $X = \sqrt{1-\sin b_{\rm g}}\cos\ell_{\rm g}$ and $Y = \sqrt{1-\sin b_{\rm g}}\sin\ell_{\rm g}$ (Lambert's zenithal equal area projection). Using the online table of globular cluster data provided by Harris (1996), we show the polar paths of some objects possibly associated with the Orphan Stream in Figure 8. The pole of the Orphan Stream lies at $(X \approx 0.31, Y \approx 0.28)$ and is marked as the filled circle. It is close to the intersections of Ruprecht 106, Palomar 1, Arp 2, Terzan 7 and the recently discovered Segue 1 (Belokurov et al. 2006c). Pal 1 and Rup 106 have often been noted as peculiar. Both are young halo globular clusters. From isochrone fitting, Rosenberg et al. (1998) estimated that Pal 1 has an age of between 6.3 and 8 Gyr and a metallicity [Fe/H] $\approx -0.6 \pm 0.2$. Rup 106 is also younger than typical halo globular clusters, by about 3 to 5 Gyr, and is very metal poor (Francois et al. 1997). Pritzl, Venn & Irwin (2005) noted that its $\alpha$ element ratios are significantly lower than Galactic field stars of similar metallicity. The anomalous properties of Rup 106 had earlier led Lin & Richer (1992) to propose that it had been accreted from the Large Magellanic Cloud. Although this is probably not the case, the idea that the young halo globular clusters may have been accreted from elsewhere – possibly from now defunct dwarf galaxies – has occurred to a number of investigators (e.g., Lynden-Bell & Lynden-Bell 1995; van den Bergh 2000; Pritzl, Venn & Irwin 2005). Terzan 7 and Arp 2 are also young halo globular clusters (Buonanno et al. 1994), but their association with the Orphan Stream seems more speculative. Both have already been claimed as part of the Sagittarius stream on the basis of distance, kinematics and chemical composition (see e.g., Sbordone et al. 2005).

## 7. CONCLUSIONS AND SUMMARY

The Orphan Stream is a $\sim 50°$ arc of stars that was detected in the Field of Streams by Belokurov et al. (2006b). It was also discovered in public SDSS data by Grillmair (2006), who applied a matched filter technique to build a color-magnitude diagram and used this to estimate the average heliocentric distance. His analysis is based on a good match between the stellar population of the Orphan Stream and the globular cluster M13. In this paper, we have presented and analyzed new observational data on the Orphan Stream, providing continuous coverage of the Stream through the area where it crosses the Sagittarius stream.

We carried out a detailed analysis of the available photometric data and used it to study the stellar populations in the Stream. Both theoretical isochrones and observational data on three globular clusters – M92, M13 and M71 – were used to build CMD masks. There is a degeneracy between age, metallicity and distance which cannot be broken with the existing photometric data. However, there is a strong indication that the stellar content of the Stream is old and metal-poor – similar to, but not identical to, the globular clusters M92 and M13. A search for blue horizontal branch population was carried out. Although this did not yield a positive detection, nonetheless there appears to be a possible blue straggler population that is associated with the Stream.

We presented evidence for the detection of a distance gradient along the Stream. The low declination fields are at a heliocentric distance of $20^{+7}_{-5}$ kpc. At higher declinations, the Stream moves farther away from us. The last photometric detection of the Stream is at $32^{+15}_{-12}$ kpc. This is close to the estimated distance of the newly-discovered dwarf spheroidal galaxy UMa II, suggesting that the Orphan Stream may be physically associated with it. Fellhauer et al. (2006) have recently carried out N body simulations of the disruption of UMa II and show that its tidal tails match the observational data available on the Orphan Stream.

Kinematic data can play a crucial role in understanding the nature of the Orphan Stream. Accordingly, we searched the spectroscopic database associated with SDSS DR5. This provides radial velocities for only about $\sim 2\%$ of all the stars in DR5. Even though there are very few candidate Orphan Stream stars with spectroscopic data, we have detected a tentative velocity signal in two fields. At the celestial equator, the stream is moving towards us at $\sim 40$ kms$^{-1}$. At high declinations, it is moving away from us at $\sim 100$ kms$^{-1}$.

The Orphan Stream lies on the same great circle as Complex A, a linear association of High Velocity Clouds, as well as a number of globular clusters, including Ruprecht 106 and Palomar 1. The recently discovered extended globular cluster Segue 1 is also very close in position and distance. All this is consistent with a picture in which a satellite galaxy merged with the Milky Way long ago. In this scenario, the Orphan Stream, UMa II, and the young halo globular clusters were torn off as tidal debris during the merging. Complex A could be neutral gas that was stripped from a gas-rich dwarf irregular progenitor, perhaps at a disk-crossing. Alternatively, a large galaxy can shock and compress ionised gas in the halo, which can then cool (Kaplan 1966), leaving a trail of neutral gas in its wake. If so, then the progenitor must have been massive, with a mass well in excess of the total mass of Complex A, which is $\sim 10^5 M_\odot$.

We particularly wish to thank Bart Wakker and James Clem for sending us data on Complex A and M92 respectively. Funding for the SDSS and SDSS-II has been provided by the Alfred P. Sloan Foundation, the Participating Institutions, the National Science Foundation, the U.S. Department of Energy, the National Aeronautics and Space Administration,

the Japanese Monbukagakusho, the Max Planck Society, and the Higher Education Funding Council for England. The SDSS Web Site is http://www.sdss.org/.

The SDSS is managed by the Astrophysical Research Consortium for the Participating Institutions. The Participating Institutions are the American Museum of Natural History, Astrophysical Institute Potsdam, University of Basel, Cambridge University, Case Western Reserve University, University of Chicago, Drexel University, Fermilab, the Institute for Advanced Study, the Japan Participation Group, Johns Hopkins University, the Joint Institute for Nuclear Astrophysics, the Kavli Institute for Particle Astrophysics and Cosmology, the Korean Scientist Group, the Chinese Academy of Sciences (LAMOST), Los Alamos National Laboratory, the Max-Planck-Institute for Astronomy (MPIA), the Max-Planck-Institute for Astrophysics (MPA), New Mexico State University, Ohio State University, University of Pittsburgh, University of Portsmouth, Princeton University, the United States Naval Observatory, and the University of Washington.

## REFERENCES

Adelman-McCarthy, J. K., et al. 2006, ApJS, 162, 38
Adelman-McCarthy, J. K., et al. 2006, ApJS, submitted.
Allende Prieto, C. et al. 2006, ApJ, 636, 804
Beers, T.C., et al. 2006, in "Exploiting Large Surveys for Galactic Astronomy", 26th meeting of the IAU, Joint Discussion 13, in press
Belokurov, V. , Evans, N. W., Gilmore, G., Hewett, P. C., Wilkinson, M. I. 2006a, ApJ, 637, L29
Belokurov, V. et al. 2006b, ApJ, 642, L137
Belokurov, V. et al. 2006c, ApJ, in press (astro-ph/0608448)
Buonanno R., Corsi C.E., Fusi Pecci R., Richer H.B., Fahlman G. 1990, ApJ, 430, L121
Clem, J. L. 2005, PhD Thesis, University of Victoria (available at http://www.phys.lsu.edu∼jclem/)
Dinescu D.I., Majewski S.R., Girard T.M., Cudworth K.M., 2001, AJ, 122, 1916
Fellhauer M., et al. 2006, MNRAS, submitted (astro-ph/0611157)
Francois P., Danziger J., Buoananno R., Perrin M.N., 1997, AA, 327, 121
Fukugita, M., Ichikawa, T., Gunn, J. E., Doi, M., Shimasaku, K., & Schneider, D. P. 1996, AJ, 111, 1748
Girardi, L., Grebel, E. K., Odenkirchen, M., & Chiosi, C. 2004, A&A, 422, 205
Grillmair C.J., Dionatos O., 2006, ApJ, 643, L17
Grillmair C.J., 2006, ApJ, 645, L37
Gunn, J.E. et al. 2006, AJ, 131, 2332
Harris W.E. 1996, AJ, 112, 1487
Hogg, D.W., Finkbeiner, D.P., Schlegel, D.J., Gunn, J.E. 2001, AJ, 122, 2129
Ibata, R. A., Irwin, M. J., Lewis, G. F., Ferguson, A. M. N., & Tanvir, N. 2003, MNRAS, 340, L21
Ivezić, Ž. et al., 2004, AN, 325, 583
Lin D.N.C, & Richer H.B. 1992, ApJ, 388, 97
Kaplan S., 1966, Interstellar Gas Dynamics, (Pergamon, Oxford)
Lupton, R., Gunn, J., & Szalay, A. 1999, AJ, 118, 1406
Lynden-Bell, D., Lynden-Bell, R. 1995, MNRAS, 275, 429
Odenkirchen, M., et al. 2001, ApJ, 548, L165
Newberg, H. J., et al. 2002, ApJ, 569, 245
Penarrubia, J., et al. 2005, ApJ, 626, 128
Pier, J.R., Munn, J.A., Hindsley, R.B, Hennessy, G.S., Kent, S.M., Lupton, R.H., Ivezic, Z. 2003, AJ, 125, 1559
Pritzl B., Venn K., Irwin M. 2005, AJ, 130, 2140
Rocha-Pinto, H. J., Majewski, S. R., Skrutskie, M. F., Crane, J. D. 2003, ApJ, 594, L115
Rosenberg A., Saviane I., Piotto G., Aparicio A., Zaggia S.R. 1998, ApJ, 115, L648
Sbordone L., Bonifacio P., Marconi G., Buonanno R., Zaggia S. 2005, AA, 437, 905
Schlegel, D.,Finkbeiner, D., & Davis, M. 1998, ApJ, 500, 525
Sivarani, T., et al. 2005, BAAS, 37, 1379
Smith J.A., et al. 2002, Aj, 123, 2121
Stoughton, C. et al. 2002, AJ, 123, 485
Wakker, B. 2001, ApJS, 136, 463
Wakker B., Howk C., Schwarz, U., van Woerden, H., Beers, T., Wilhelm, R., Kalberla, P., & Danly, L. 1996, ApJ, 473, 834
van Woerden, H., Schwarz, U. J., Peletier, R. F., Wakker, B. P., Kalberla, P. M. W. 1999, Nat, 400, 138
Yanny B., et al 2003, ApJ, 588, 824
York D.G., et al. 2000, AJ, 120, 1579
van den Bergh S. 2000, AJ, 112, 529
Zucker D., et al. 2006, ApJ, 650, L41